

Research article

Open Access

POU-domain factor Brn3a regulates both distinct and common programs of gene expression in the spinal and trigeminal sensory ganglia

S Raisa Eng, Iain M Dykes, Jason Lanier, Natalia Fedtsova and Eric E Turner*

Address: Department of Psychiatry, University of California, San Diego and VA San Diego Healthcare System, Gilman Drive, La Jolla, CA 92093-0603, USA

Email: S Raisa Eng - sreng@ucsd.edu; Iain M Dykes - idykes@ucsd.edu; Jason Lanier - jlanier@ucsd.edu; Natalia Fedtsova - nfedtsova@ucsd.edu; Eric E Turner* - eturner@ucsd.edu

* Corresponding author

Published: 19 January 2007

Received: 4 November 2006

Neural Development 2007, **2**:3 doi:10.1186/1749-8104-2-3

Accepted: 19 January 2007

This article is available from: <http://www.neuraldevelopment.com/content/2/1/3>

© 2007 Eng et al; licensee BioMed Central Ltd.

This is an Open Access article distributed under the terms of the Creative Commons Attribution License (<http://creativecommons.org/licenses/by/2.0>), which permits unrestricted use, distribution, and reproduction in any medium, provided the original work is properly cited.

Abstract

Background: General somatic sensation is conveyed to the central nervous system at cranial levels by the trigeminal ganglion (TG), and at spinal levels by the dorsal root ganglia (DRG). Although these ganglia have similar functions, they have distinct embryological origins, in that both contain neurons originating from the neural crest, while only the TG includes cells derived from the placodal ectoderm.

Results: Here we use microarray analysis of E13.5 embryos to demonstrate that the developing DRG and TG have very similar overall patterns of gene expression. In mice lacking the POU-domain transcription factor Brn3a, the DRG and TG exhibit many common changes in gene expression, but a subset of Brn3a target genes show increased expression only in the TG. In the wild-type TG these Brn3a-repressed genes are silent, yet their promoter regions exhibit histone H3-acetylation levels similar to constitutively transcribed gene loci. This increased H3-acetylation is not observed in the DRG, suggesting that chromatin modifications play a role in cell-specific target gene regulation by Brn3a.

Conclusion: These results demonstrate that one developmental role of Brn3a is to repress potential differences in gene expression between sensory neurons generated at different axial levels, and to regulate a convergent program of developmental gene expression, in which functionally similar populations of neurons are generated from different embryological substrates.

Background

The generation of cellular diversity in the developing vertebrate nervous system is one of the most complex problems in biology, and a large number of transcription factors have been identified that orchestrate neurodevelopment and regulate the molecular identity of neurons. Perhaps the best-studied systems for the establishment of

neuronal phenotypes in vertebrates are the primary input (sensory) and output (motor) pathways of the peripheral sensory ganglia, spinal cord, and brainstem. In these areas, several key transcriptional regulators have been identified, many of which are members of the basic-helix-loop-helix (bHLH) and homeodomain transcription factor classes [1,2].

The peripheral sensory nervous system is organized anatomically according to the nature of the external information reported to the central nervous system (CNS). The sensory modalities of pain, touch, temperature and proprioception are transduced by sensory neurons innervating the skin and musculoskeletal structures, and are referred to as general somatic sensation. Peripheral sensory neurons also convey the senses of taste and hearing, and visceral sensation, which reports the state of the internal organs. At spinal levels, general somatic sensation is conveyed by the dorsal root or spinal ganglia (DRG), while in the anterior head and face, these sensory modalities are mediated by the trigeminal ganglion (TG).

Surprisingly, in spite of the similar functions of the DRG and TG, these ganglia have rather different embryological origins. The DRG are formed entirely from spinal neural crest. In contrast, the TG is formed in part from the ophthalmic and maxillo-mandibular placodes originating in the surface ectoderm, as well as cranial neural crest cells derived from rhombomere 2, which migrate and condense to form the ganglion [3,4]. The trigeminal system also includes a population of sensory neurons that reside outside the anatomical ganglion, the mesencephalic trigeminal (mesV), the exact origin of which is still somewhat controversial [5,6]. The developmental mechanisms that lead to the differentiation of functionally similar populations of neurons from these different embryological sources are not well understood.

Transcriptional regulators of sensory development may be broadly divided into early factors that are essential for neurogenesis, pan-sensory factors that begin to be expressed around the time of cell-cycle exit, and late factors that characterize specific sensory subtypes. In mice, the proneural bHLH factors Ngn1 and Ngn2 are expressed transiently from embryonic day 8.5 in cranial sensory precursors and have been shown to have a crucial role in neurogenesis [7-9]. Around the time of ganglion condensation and cell cycle exit, beginning at E9.5-10.5, nearly all sensory neurons at both spinal and cranial levels co-express the homeodomain transcription factors Brn3a and Islet1 [1,10]. Later in development, factors associated with the development of specific sensory subtypes include the runt family factors Runx1 and Runx3, the variant homeodomain protein Prrx1/DRG11, and the Ets family member Etv1/Er81 [1,11-15].

Studies of Brn3a knockout mice have shown that this factor is required for correct axon growth, target innervation, and survival of TG and DRG neurons [16-19]. Microarray studies of the developing TG of Brn3a null mice have shown that Brn3a is required for a complex program of sensory gene expression [20]. In the present study, we examine the role of Brn3a in sensory neurogenesis at trun-

cal and cranial levels. In normal mice, the developing DRG and TG have very similar patterns of global gene expression. The loss of Brn3a expression in the developing DRG leads to marked changes in the expression of specific neurotransmitters, receptors, developmental regulators, mediators of signal transduction, and transcription factors. Many of these changes are conserved between the TG and DRG of Brn3a knockout mice, but certain transcripts are markedly increased only in the cranial ganglia. The promoter regions of these normally silent but differentially regulated genes are hyperacetylated only in the TG, which may indicate a latent state of 'expressability' that can differ between spinal and cranial levels. Thus, a key developmental role of Brn3a may be to repress potential differences in gene expression between developing DRG and TG neurons, and thus promote the generation of functionally similar populations of neurons from different embryological sources.

Results

Global gene expression is highly conserved in sensory neurons from different axial levels

To begin to compare the molecular program of sensory neuron development at spinal and cranial levels, we performed global analysis of gene expression in the developing DRG and TG. E13.5 was chosen for this comparison because, at this stage, most of the neurons of the DRG and TG have exited the cell cycle and have begun to express definitive markers of neurogenesis. Because sensory neurons have conserved functions at spinal and cranial levels, we hypothesized that the global pattern of gene expression in the DRG would be much more similar to the TG than to other neural tissues. Figure 1 illustrates a comparison of gene expression in the DRG to a replicate analysis from the same tissue, to the TG, and to the embryonic neocortex. These results show a high degree of overall similarity in gene expression between the sensory ganglia from different axial levels, and confirm that there is much greater divergence between the patterns of gene expression in the DRG and the developing cerebral cortex.

Overall, only a very small fraction of the approximately 44,000 transcripts assayed by the array showed profound differences in expression between the DRG and TG (Table 1). Significantly more transcripts were uniquely expressed in the DRG, and seven out of ten of the transcripts with the highest relative expression in the DRG encoded Hox transcription factors, an expected finding given the axial restriction of Hox expression. Several of the other differentially expressed genes revealed in the microarray analysis could be validated by *in situ* hybridization (see additional file 1), although some differences appear to represent anomalous findings that may be related to factors such as high expression in peripheral glia (Ednrb, Sostdc1).

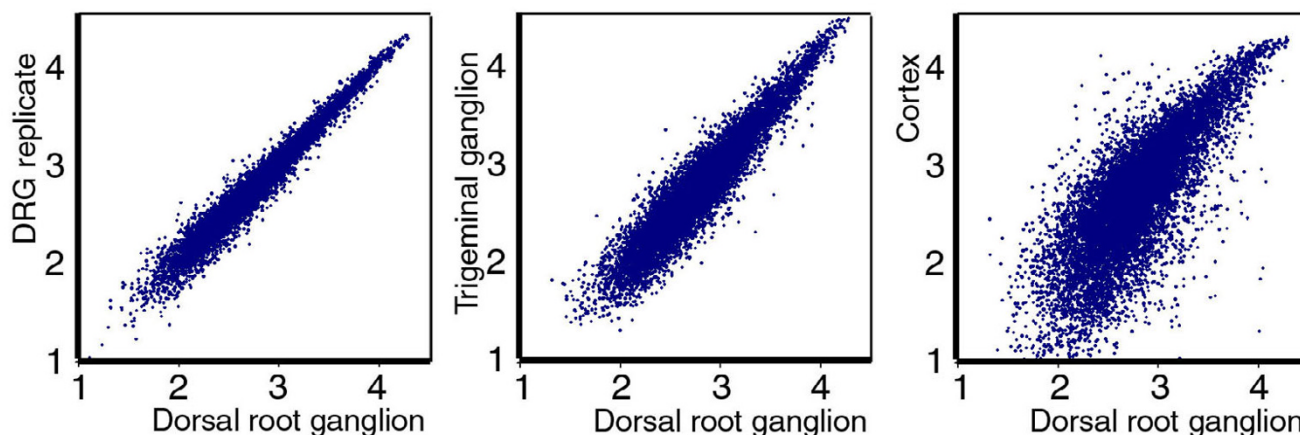


Figure 1

Analysis of global gene expression in embryonic neural tissue. Analysis of global gene expression was performed using E13.5 DRG, E13.5 TG and E16.5 cerebral cortex samples. Only probe sets on the Affymetrix 430A array are shown, and transcripts with 'absent' calls in all three samples were excluded from the analysis. **(a)** Plot of DRG expression versus a replicate DRG assay closely approximates a diagonal line indicating equal expression in the two samples. **(b)** Plot of DRG expression versus the TG indicates very similar global gene expression in the two samples, with few points lying far from the diagonal. **(c)** Plot of DRG expression versus the embryonic cerebral cortex indicates a large number of transcripts that are differentially expressed between the two samples. Axis is graduated in log₁₀ of scaled signal.

Aside from the Hox factors, the transcript with the greatest relative expression in the DRG was *Etv1*, an Ets-family transcription factor expressed in 1a muscle spindle afferents [13,21]. Immunofluorescence for *Etv1* expression in the E13.5 DRG confirmed expression in sensory neurons of large and intermediate size, whilst expression was entirely absent in the TG at this stage (Figure 2a, b). In contrast, expression of *Runx3*, an earlier and more general marker of proprioceptive neurons [13,14], was noted in both the DRG and TG at E13.5 (Figure 2c, d).

By E16.5, *Etv1* expression could be detected in some neurons of the TG, as well as the DRG. In the DRG, one population of *Etv1*-expressing neurons displayed large soma and nuclei consistent with 1a proprioceptors. However, in the TG nearly all of the *Etv1*-expressing neurons were of intermediate size, and large *Etv1*-positive neurons consistent with 1a proprioceptors were rare. In both the DRG and the TG, this intermediate-sized and later-developing population of *Etv1*-expressing sensory neurons could be further distinguished from the 1a proprioceptors by the co-expression of *Islet2* (Figure 2e, f).

One distinguishing feature of the TG is that a subset of neurons that are functionally part of the trigeminal system, the mesV, is located within the CNS. Examination of the mesV in late gestation revealed large sensory neurons positive for *Etv1*. These neurons co-expressed a *tauLacZ* transgene integrated into the *Brn3a* locus, and *Brn3a* is a known marker of the mesencephalic trigeminal [6]. The

position of these neurons in the caudal midbrain is consistent with the role of some of these neurons as muscle spindle afferents for the muscles of mastication [22]. Thus, the exclusive expression of *Etv1* in the DRG but not the TG at E13.5 appears to result from a population of *Etv1*⁺, *Islet2*⁻ proprioceptive neurons that are present in the DRG but are largely restricted to the mesV at the cranial level.

***Brn3a* regulates multiple downstream targets in the DRG**

To understand the developmental programs regulated by *Brn3a* at spinal versus cranial levels, we next analyzed global gene expression in E13.5 DRG from *Brn3a* mutant embryos and wild-type controls. Tables 2 and 3 summarize the transcripts most increased and decreased at E13.5 in the DRG of *Brn3a* knockout mice, and a more complete list appears in additional file 2. *In situ* hybridization and immunofluorescence were used to verify altered expression of several of the target genes (Figures 3 and 4), with an emphasis on newly identified *Brn3a* targets and genes for which expression has not been previously described in the sensory ganglia.

Most of the *Brn3a*-regulated genes of known function have specific roles in neurotransmission, axonogenesis/synaptogenesis, signal transduction, regulation of developmental pathways, or transcription. Among mediators of neurotransmission, multiple glutamate receptors (*Gria3*, *Gria4*, *Grik1*), a GABA transporter (*Slc6a1*), a serotonin receptor (*Htr3a*) and the neuropeptide somato-

Table 1: Transcripts differentially expressed in the DRG and TG

| Transcript | Symbol | Class | Fold |
|---|--------------------|-------|--------|
| Greater expression in the DRG | | | |
| Homeobox B3 | Hoxb3 ² | TX | (90.4) |
| Homeobox A9 | Hoxa9 | TX | (90.2) |
| Homeobox A5 | Hoxa5 ² | TX | (44.2) |
| Etv1; ER81 | Etv1 ³ | TX | (40.2) |
| Homeobox C8 | Hoxc8 ² | TX | (38.4) |
| Homeobox B6 | Hoxb6 | TX | (27.6) |
| Hoxd4 | Hoxd4 | TX | (16.6) |
| Follistatin | Fst ² | Dev | (12.9) |
| Leucine-rich repeat-containing G protein-coupled receptor 6 | Lgr6 | Other | (11.8) |
| Receptor (calcitonin) activity modifying protein 2 | Ramp2 ³ | ST | 10.9 |
| Ca ⁺ channel, L type, alpha 1C subunit | Cacna1c | NT | 9.2 |
| Homeobox B8 | Hoxb8 | TX | (9.1) |
| BTB and CNC homology 2 | Bach2 | TX | (8.8) |
| Sclerostin domain containing 1 | Sostdc1 | Dev | 8.5 |
| Laminin, alpha 2 | Lama2 | Other | (7.3) |
| Selected | | | |
| Purkinje cell protein 4 | Pcp4 | Unk | (5.7) |
| LIM domain binding 2 | Ldb2 ² | TX | 5.6 |
| Zinc finger protein of the cerebellum 1 | Zic1 ² | TX | 5.3 |
| Gap junction membrane channel protein alpha 1 | Gja1 ² | NT | 5.1 |
| Protein tyrosine phosphatase, receptor type, E | Ptpre3 | ST | 5.0 |
| Early B-cell factor 1; Olf1 | Ebfl | TX | 5.0 |
| U74 array | | | |
| Regulator of G-protein signaling 4 | RGS4 | NT | 6.1 |
| Endothelin receptor type B | EDNRB | Other | 3.0 |
| Anthrax toxin receptor 2 | Antxr2 | Unk | 3.0 |
| Greater expression in the TG | | | |
| Microfibrillar-associated protein 4 | Mfap4 | Unk | (20.6) |
| Lectin, galactose binding, soluble 7 | Lgals7 | AX | (11.3) |
| MyoD family inhibitor | Mdfi | TX | (9.6) |
| Suppressor of cytokine signaling 3 | Socs3 ² | ST | (6.4) |
| RNA imprinted and accumulated in nucleus | Rian | Unk | 6.1 |
| Musashi homolog 2 | Msi2h | Other | 6.0 |
| U74 array | | | |
| Neuropeptide Y receptor 1 | NpyR1 | NT | 8.6 |

The principal analysis was conducted with the murine 430 array, with selected results identified using the U74A+B array set added. All listed transcripts showed increased expression (change $p < 0.005$) in two independent replicates. Fold values represent the ratio of the means of two determinations for each tissue. Fold changes in parentheses indicate an absent call, that is, below the statistically reliable limit of detection, in the lower expressing sample. Transcripts with expression levels less than 40% of the scaled mean are excluded. Superscript numerals represent the number of probe sets concordant for changed expression for a given gene. AX, axonogenesis; Dev, development; NT, neurotransmission; ST, signal transduction; Syn, synaptogenesis; TX, transcription; Unk, unknown. Greater expression in the DRG: confirmation of selected results by *in situ* hybridization and immunofluorescence appears in additional file 1. Differential expression of Ramp2 could not be confirmed by ISH. Different levels of Zic1 and follistatin appear to be due to high expression in the spinal cord adjacent to the DRG, rather than the DRG itself. Sostdc1 and EDNRB showed increased DRG expression by ISH but in a pattern more characteristic of glial than neuronal expression, with signal concentrated in nerve roots. The expression of RGS4 in the developing sensory ganglia has been previously described [43], and its higher expression in the DRG at E13.5 appears to be due to the dynamic developmental regulation of this gene, rather than a persisting difference in expression between the DRG and TG. Greater expression in the TG: *in situ* hybridization confirmed some changes (see additional file 1). However, Mfap4 was widely expressed in embryonic tissues. Socs3 ISH exhibited relatively greater expression in the TG, but overall expression levels were low. Differential expression of the suppressor of cytokine signaling Socs3 in the TG and DRG has previously been noted [44].

statin are increased, while a GABA receptor (Gabra2) and neuropeptides with specific sensory roles (Galanin, Adcyap1/PACAP) are decreased. Also reduced is latexin, a secreted carboxypeptidase inhibitor with a role in nociception [23].

Profound changes were also observed in genes that encode known or potential mediators of sensory neurogenesis, and axon growth or guidance. Increased transcripts in this class included the cell adhesion molecule Chl1, which has a known role in the growth of cortical

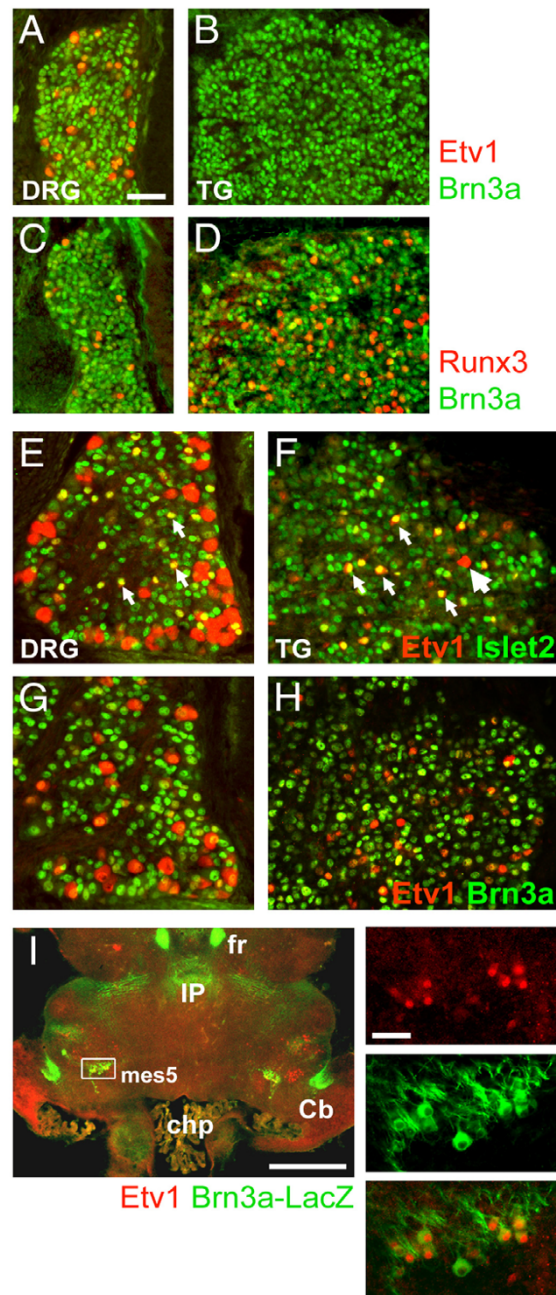


Figure 2

Selective expression of proprioceptor markers in the DRG and trigeminal system. The sensory ganglia of wild-type embryos were examined at E13.5 and E16.5 for the expression of transcription factors Brn3a, Etv1, Runx3 and Islet2. **(a-d)** At E13.5, Etv1 expression is restricted to the DRG, while Runx3 is expressed in both the DRG and TG. **(e-h)** At E16.5, Etv1 is expressed in both the DRG and the TG, but in the TG Etv1 positive neurons with large nuclei consistent with Ia proprioceptors are rare (large arrow). Instead, the majority of Etv1-positive neurons in the TG have nuclei of intermediate size and co-express Islet2; similar cells are also found in the DRG (small arrows). The Ia proprioceptors of the DRG co-express Brn3a, but at relatively low levels. **(i)** Etv1 expression in the mesV of an E18.5 embryo expressing a *tauLacZ* transgene integrated into the Brn3a locus [42], which is thus heterozygous for Brn3a, but phenotypically normal. Numerous neurons that co-express Etv1 and the Brn3a-LacZ marker are noted. The caudal location and large size of these neurons are consistent with proprioceptors innervating the muscles of mastication. Cb, cerebellum; chp, choroid plexus; fr, fasciculus retroflexus; IP, interpeduncular nucleus; mes5, mesencephalic trigeminal. Scale 50 μ m (a-h), 400 μ m (i), 50 μ m (i, inset).

Table 2: Increased transcripts in the DRG of Brn3a knockout mouse

| Transcript | Symbol | Class | WT | HT | KO | KO/WT |
|--|----------------------|-------|-------|-------|-------|-------|
| Chordin-like 1 | Chrdl1 | Dev | 5 | 2 | 134 | 27.4 |
| Musculin (MyoR) | Msc | TX | 211 | 675 | 1,260 | 6.0 |
| Insulinoma-associated 1 | Insm1 ² | TX | 153 | 301 | 827 | 5.4 |
| GABA transporter 1 (Gabt1) | Slc6a1 | NT | 74 | 93 | 397 | 5.3 |
| Microfibrillar-associated 4 | Mfap4 | Unk | 112 | 370 | 559 | 5.0 |
| Secretogranin II | Scg2 | SY | 206 | 253 | 966 | 4.7 |
| C-fos induced growth factor (VEGF-D) | Figf | Dev | 76 | 102 | 319 | 4.2 |
| Guanylate cyclase 1, alpha 3 | Gucy1a3 | ST | 50 | 82 | 205 | 4.1 |
| Neurogenic differentiation 6 (Math2, Nex) | Neurod6 | TX | 83 | 200 | 344 | 4.1 |
| Somatostatin | Sst | NT | 215 | 382 | 830 | 3.9 |
| Neurexin III | Nrxn3 ⁴ | SY | 367 | 961 | 1,412 | 3.8 |
| Bruno-like 4 | Bruno14 ³ | Other | 154 | 274 | 588 | 3.8 |
| Cell adhesion molecule with homology to LICAM | Chl1 | AX | 128 | 127 | 466 | 3.6 |
| Junctophilin 1 | Jph1 | Other | 74 | 119 | 262 | 3.5 |
| Glutamate receptor, ionotropic, AMPA4 | Gria4 ³ | NT | 46 | 80 | 161 | 3.5 |
| Glutamate receptor, ionotropic, AMPA3 | Gria3 | NT | 40 | 66 | 138 | 3.5 |
| Zinc finger homeobox 1b | Zfx1b ² | TX | 81 | 127 | 270 | 3.3 |
| Nel-like 2 | Nell2 | AX | 383 | 331 | 1,215 | 3.2 |
| Follistatin-like 5 | Fstl5 ² | Dev | 281 | 389 | 885 | 3.2 |
| Disabled homolog 1 | Dab1 ² | AX | 90 | 42 | 272 | 3.0 |
| Mannan-binding lectin serine protease 1 | Masp1 | Other | 95 | 101 | 282 | 3.0 |
| Selected | | | | | | |
| Semaphorin 3C | Sema3c ² | AX | 589 | 723 | 1,732 | 2.9 |
| Cholecystokinin A receptor | Cckar | NT | 95 | 161 | 269 | 2.8 |
| Serotonin receptor 3A | Htr3a | NT | 778 | 1,160 | 2,090 | 2.7 |
| Homeobox A5 | Hoxa5 | TX | 628 | 896 | 1,493 | 2.4 |
| Neurogenic differentiation 1 | Neurod1 ² | TX | 1,048 | 1,468 | 2,440 | 2.3 |
| p21-activated kinase 3 | Pak3 ² | SY | 246 | 270 | 568 | 2.3 |
| Semaphorin 3D | Sema3d | AX | 318 | 365 | 725 | 2.3 |
| Protocadherin 17 | Pcdh17 ² | AX | 331 | 340 | 746 | 2.3 |
| Spondin 1, (f-spondin) | Spon1 | AX | 629 | 778 | 1,413 | 2.2 |
| K ⁺ voltage-gated channel, Isk family | Kcne11 | NT | 613 | 813 | 1,328 | 2.2 |
| Deleted in colorectal carcinoma | Dcc | AX | 93 | 101 | 200 | 2.2 |
| Netrin G1 | Ntng1 | AX | 388 | 556 | 812 | 2.1 |
| Neuropilin 2 | Nrp2 | AX | 509 | 485 | 1,063 | 2.1 |
| Cadherin 22 | Cdh22 | AX | 199 | 226 | 414 | 2.1 |
| Synapsin II | Syn2 ⁴ | SY | 643 | 688 | 1,324 | 2.1 |
| Glutamate receptor, ionotropic, kainate 1 | Grik1 | NT | 221 | 241 | 455 | 2.1 |
| Protocadherin 8 | Pcdh8 ² | AX | 278 | 398 | 569 | 2.0 |
| GDNF receptor alpha 2 | Gfra2 | Dev | 363 | 436 | 735 | 2.0 |
| Nescient helix loop helix 2 (Nsc12) | Nhlh2 | TX | 1,222 | 1,996 | 2,446 | 2.0 |

Data for one of two independent experiments are shown. All listed transcripts showed increased expression (change $p < 0.005$) in two independent replicates. Data are complete for all replicated changes above three-fold, and selected data appear for transcripts exhibiting two- to three-fold change. A full data set appears in Additional file 1. Superscript numerals represent the number of probe sets concordant for changed expression for a given gene. AX, neurogenesis/axon growth and guidance; Dev, development; KO, knockout; NT, neurotransmission; ST, signal transduction; SY, synapse formation and function; TX, transcription; Unk, unknown; WT, wild type.

dendrites [24], and Nel-like 2, an epidermal growth factor (EGF)-repeat containing factor with a previously demonstrated role in sensory development [25]. Increased expression was also noted for several molecules with known or likely roles in axon guidance, including Disabled1, Sema3c, Sema3d, f-spondin, Cadherin22, Protocadherin 8, Protocadherin 17, Dcc, and NetrinG1. Decreased expression was noted for advillin, an actin binding protein that is a known mediator of sensory neu-

rite outgrowth [26], as well as Ncam2 and Eph receptor A7. These changes suggest that the profound defects observed in the sensory axons of Brn3a null mice [17] result from the derangement of a coordinated program of expression of mediators of axon growth and guidance, rather than from a single molecular lesion.

Loss of Brn3a also resulted in significant changes in the expression of other transcription factors. Notably, dele-

Table 3: Transcripts decreased in the DRG of Brn3a null mice

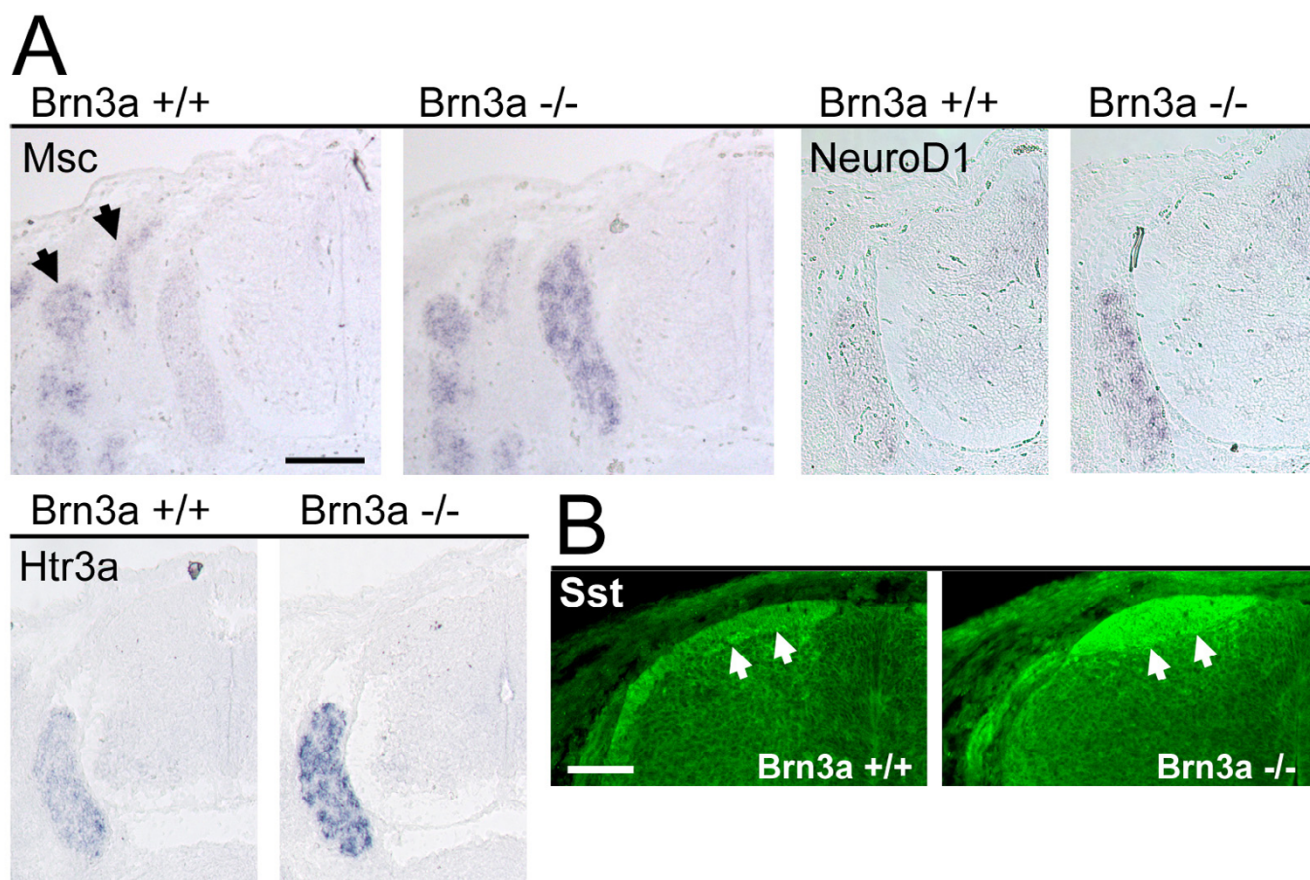
| Transcript | Symbol | Class | WT | HT | KO | WT/KO |
|--|---------------------|-------|-------|-------|-------|-------|
| Limb expression 1 | Lix1 | Unk | 984 | 923 | 46 | 21.4 |
| Vascular endothelial growth factor C | Vegfc | Dev | 55 | 54 | 3 | 16.1 |
| Neural cell adhesion molecule 2 | Ncam2 ² | AX | 280 | 212 | 22 | 12.9 |
| Runt related 3 | Runx3 | TX | 251 | 421 | 22 | 11.3 |
| Brn3b | Pou4f2 | TX | 613 | 772 | 61 | 10.0 |
| Brn3a | Pou4f1 ² | TX | 1,107 | 1,119 | 115 | 9.6 |
| Phospholipase A2, group VII | Pla2g7 | ST | 618 | 438 | 77 | 8.1 |
| K ⁺ channel, shaker-related, member 1 | Kcna1 ³ | NT | 438 | 523 | 59 | 7.4 |
| Advillin | Avil | AX | 2,494 | 1,735 | 364 | 6.9 |
| Galanin | Gal | NT | 5,388 | 4,414 | 824 | 6.5 |
| Basonuclin 1 | Bnc1 | TX | 875 | 740 | 165 | 5.3 |
| Insulin-like growth factor 1 | Igf1 ³ | Dev | 820 | 609 | 160 | 5.1 |
| G protein-coupled receptor 64 | Gpr64 ² | NT | 371 | 298 | 72 | 5.1 |
| Adenylate cyclase activating polypeptide 1, PACAP | Adcyap1 | NT | 283 | 198 | 57 | 5.0 |
| Regulator of G-protein signaling 10 | Rgs10 | NT | 1,793 | 1,596 | 362 | 5.0 |
| Parvalbumin | Pvalb | ST | 403 | 223 | 95 | 4.3 |
| K ⁺ channel, shaker-related, beta member 2 | Kcnab2 | NT | 952 | 684 | 238 | 4.0 |
| Diacylglycerol kinase, eta | Dgkh ² | ST | 1,348 | 1,230 | 353 | 3.8 |
| G protein-coupled receptor 73 | Gpr73 | NT | 336 | 157 | 90 | 3.7 |
| Serine proteinase inhibitor, clade A, member 3G; Spi2A | Serpina3g | Other | 426 | 346 | 116 | 3.7 |
| Copine IV | Cpne4 | Unk | 767 | 636 | 216 | 3.6 |
| PQ loop repeat containing 1 | Pqlc1 | Unk | 911 | 596 | 259 | 3.5 |
| Reticulon 4 receptor-like 2; nogo receptor-like 3 | Rtn4rl2 | AX | 789 | 694 | 226 | 3.5 |
| Spermatogenesis associated glutamate-rich protein 1 | Speer1-ps1 | Unk | 349 | 307 | 106 | 3.3 |
| Pappalysin 2 | Pappa2 | Other | 694 | 794 | 225 | 3.1 |
| Brn3c | Pou4f3 | TX | 394 | 361 | 130 | 3.0 |
| Protein tyrosine phosphatase, receptor type, J | Ptprj | ST | 853 | 918 | 284 | 3.0 |
| Docking protein 4 | Dok4 | ST | 2,014 | 1,655 | 679 | 3.0 |
| Selected | | | | | | |
| Eph receptor A7 | Epha7 | AX | 206 | 202 | 77 | 2.7 |
| Latexin | Lxn | NT? | 2,948 | 2,564 | 1,105 | 2.7 |
| DRG11 | Prrxl1 | TX | 1,514 | 1,339 | 569 | 2.7 |
| Protein tyrosine phosphatase, non-receptor type 3 | Ptpn3 | ST | 1,638 | 1,881 | 623 | 2.6 |
| GABA-A receptor, subunit alpha 2 | Gabra2 | NT | 62 | 90 | 24 | 2.6 |
| Na ⁺ channel, type VII, alpha | Scn7a | NT | 1,199 | 1,386 | 506 | 2.4 |
| Protein tyrosine phosphatase, receptor type, R | Ptpr | ST | 3,376 | 3,207 | 1,467 | 2.3 |
| Rap1, GTPase-activating protein 1 | Rap1ga1 | ST | 1,721 | 1,686 | 749 | 2.3 |
| LIM domain binding 2 | Ldb2 | TX | 794 | 492 | 349 | 2.3 |
| Anthrax toxin receptor 2 | Antxr2 | Unk | 1,355 | 1,095 | 608 | 2.2 |
| Runt related txn factor 1 | Runx1 | TX | 360 | 343 | 162 | 2.2 |
| Homeobox D1 | Hoxd1 | TX | 852 | 751 | 404 | 2.1 |
| Inhibitor of DNA binding 1 | Id1 | TX | 1,248 | 1,051 | 624 | 2.0 |

All listed transcripts showed decreased expression (change $p > 0.995$) in two independent replicates. Complete data appear for all replicated changes above three-fold, and selected data appear for transcripts exhibiting change in the two- to three-fold range. A full data set appears in Additional File 2. Note that Brn3a transcripts are still detected in the Brn3a null genotype, consistent with the detection of the 3'-end of residual non-coding transcripts. AX, neurogenesis/axon growth and guidance; Dev, development; KO, knockout; NT, neurotransmission; ST, signal transduction; SY, synapse formation and function; TX, transcription; Unk, unknown; WT, wild type.

tion of Brn3a effectively resulted in a triple-knockout of the Pou4 homeodomain class, because Pou4f2 (Brn3b) expression is nearly eliminated, and Pou4f3 (Brn3c) expression is greatly reduced in Brn3a knockout ganglia. Marked decreases were also observed in specific markers of sensory neuron subclasses, including Prrxl1/DRG11, Runx1 and Runx3. In contrast, specific bHLH genes, including those encoding NeuroD1, NeuroD6, Msc, and Nhlh2, were increased, and, perhaps consistent with this,

the inhibitory bHLH factor Id1, which can act to oppose the action of neurogenic bHLH genes, was decreased. The significance of some of these changes in the hierarchy of gene regulation in developing sensory neurons is discussed below.

Loss of Brn3a expression resulted in increased expression of essentially all of the anterior *HoxA*, *HoxB* and *HoxC* genes, and the changes reached statistical significance ($p <$

**Figure 3**

Target genes with increased expression in the DRG of Brn3a null mice. **(a)** *In situ* hybridization confirms increased expression of Msc (musculin), NeuroD1, and Htr3a (serotonin receptor 3A) transcripts in the DRG of Brn3a wild-type and knockout embryos. Note that the expression of Msc in the surrounding musculature (arrows) is unchanged. **(b)** Immunofluorescence for the somatostatin-14 peptide shows increased expression concentrated in the dorsal root entry zone (arrows). The distribution of somatostatin-14 also reveals an abnormal accumulation of axons in the superficial dorsal horn in the Brn3a null mutant. All views show lower cervical (brachial) level cross-sections of E13.5 embryos. Scale: 200 μm (a), 50 μm (b).

0.005 or $p > 0.995$, Materials and Methods) for seven genes in this group (Figure 5). The posterior *Hox* genes were expressed at much lower levels than the anterior factors, as expected for brachial-level DRG, and exhibited either unchanged or decreased expression in the knockout. Members of the *HoxD* cluster were not significantly expressed in the DRG (data not shown), with the exception of *HoxD1*, which, unlike the other anterior *Hox* gene products, exhibited decreased expression in Brn3a null DRG, and was also the only *Hox* gene product expressed at significant levels in the TG (see additional file 3) [20].

In prior studies, we have shown that Brn3a regulates its own expression via direct negative feedback, and that, in heterozygous Brn3a knockout mice, partial relief of this negative autoregulation results in increased expression of the intact allele, resulting in nearly complete gene dosage

compensation. To determine whether gene dosage compensation is also present at spinal levels, we examined the levels of all increased and decreased transcripts in Brn3a^{+/+}, Brn3a^{+/-} and Brn3a^{-/-} ganglia (see additional files 2 and 4). In each case, the mean effect of the loss of one *Brn3a* allele on target gene expression was 16% to 19% of the effect of the loss of both alleles, compared to the 50% change that would be expected without any compensatory mechanism, indicating significant but incomplete compensation for gene dosage.

A subset of Brn3a targets are unique to the cranial sensory ganglia

Comparison of the regulatory targets of Brn3a in the developing DRG with our prior analysis of the TG [20] suggests that there are many downstream genes in common between these ganglia. However, results from the

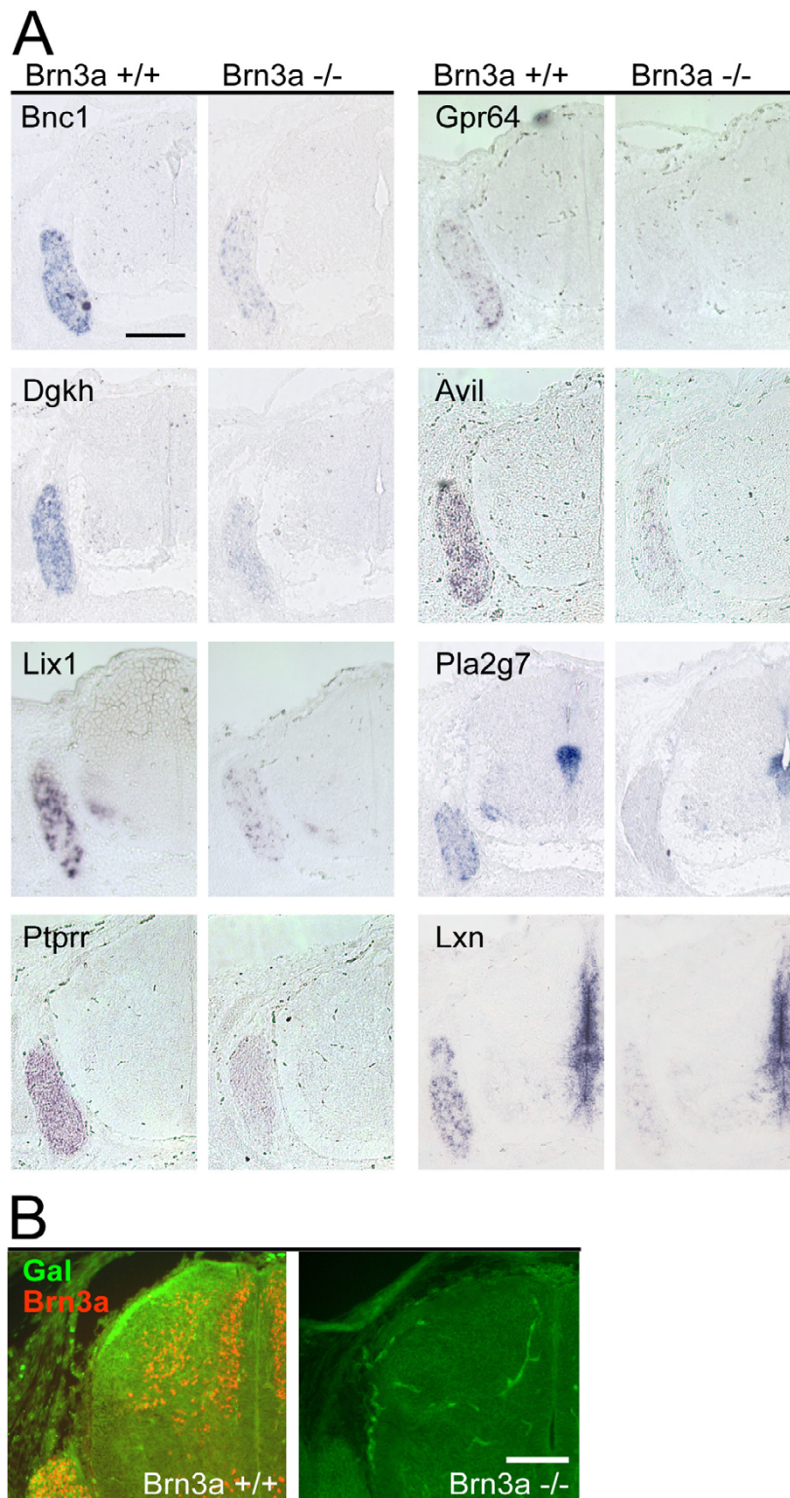
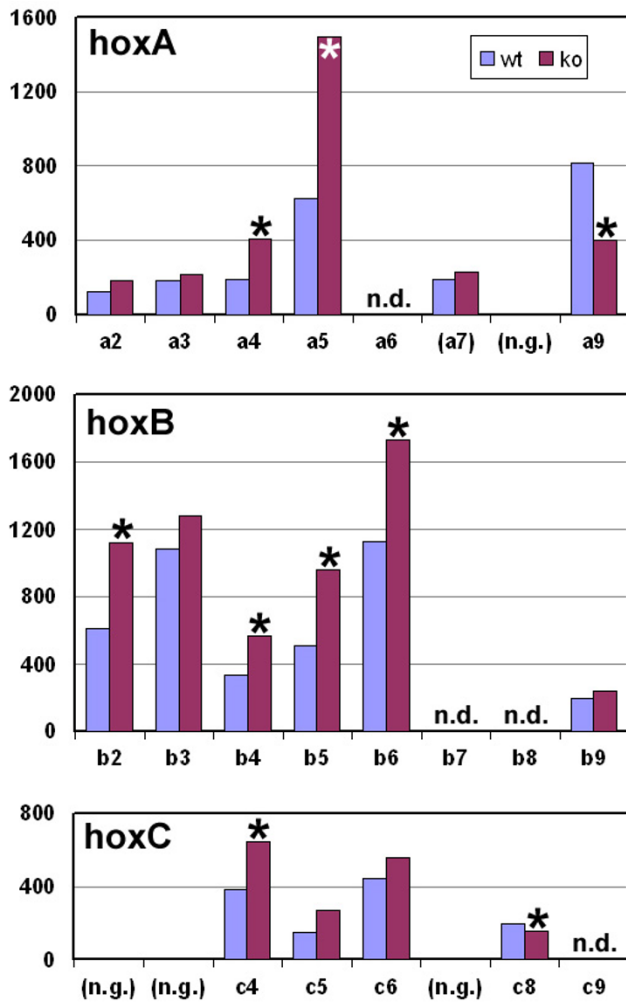


Figure 4

Target genes with decreased expression in the DRG of Brn3a null mice. **(a)** *In situ* hybridization confirms decreased expression of multiple Brn3a downstream targets. **(b)** Immunofluorescence for the galanin neuropeptide shows marked reduction in the dorsal horn and dorsal root entry zone of Brn3a null DRG. All views show lower cervical (brachial) level cross sections of E13.5 embryos. Scale: 200 μ m (a), 100 μ m (b).

**Figure 5**

Brn3a regulation of *Hox* gene expression in the DRG. *Hox* gene expression data were derived from 430A+B array data for E13.5 Brn3a wild-type (wt) and knockout (ko) DRG. Statistically significant increases ($p < 0.005$) in the knockout were observed for 7 anterior *Hox* transcripts, and significant decreases were observed ($p > 0.995$) for two posterior *Hox* transcripts (asterisks). Similar changes reached statistical significance for 5 anterior *Hox* genes and one posterior *Hox* gene in a replicate assay. *HoxA7* (parentheses) did not reach statistical significance for detection, indicating high background signal in this probe set. Legend: n.g., no gene at the corresponding position in the cluster; n.d., not determined.

more advanced microarray used in the present study (Affymetrix 430) cannot be compared directly to the prior TG data derived from an older array (Affymetrix U74v2). To make such a comparison, we performed an additional analysis of these E13.5 DRG samples with the U74v2 array. We also updated the interpretation of the results for the TG U74v2 dataset using annotations from Build 34 of the mouse genome. This analysis confirmed that the DRG

and TG of E13.5 Brn3a knockout mice have many conserved changes in gene expression (see additional file 3). Transcripts increased in both the DRG and TG of Brn3a knockout mice include the bHLH transcription factors *musculin* and *NeuroD1*, the neurotransmitters/receptors *somatostatin*, *CCK-receptor A*, *5HT-receptor 3A*, and *GABA-transporter 1*, and the growth factor *FIGF/VEGF-D*. Conserved decreases include the transcription factors *Hmx1*, *Runx1* and *basonuclin*, the peptides *galanin* and *PACAP*, as well as *advillin* and *latexin*.

Although the majority of the downstream targets of Brn3a were conserved in the DRG and TG, a subset of genes was uniquely regulated at each axial level. The most profound differences were observed for a set of genes markedly increased in the TG of Brn3a knockout embryos, and unchanged in the DRG (Figure 6). These differentially regulated genes include those encoding the transcription factors *Tcfap2b* (*Ap2β*), *NeuroD4* (*Math3*) and *Gata3*, the calcium binding protein *Calb2* (*calretinin*) and the small GTP-binding protein *Rab3b*. These results led us to consider possible mechanisms for cell-specific target gene regulation by Brn3a in these two closely related neural tissues.

The cell-type specific effects of transcription factors are generally attributed to distinct complements of interacting partners, or to the expression of related factors that provide redundancy in some cell types but not in others. However, with the exception of the *Hox* factors, the very similar gene expression profiles of the DRG and TG do not suggest many candidates for distinct Brn3a partners in these neurons. In addition, the loss of Brn3a effectively eliminates expression of all *Pou4* class factors in both the DRG and TG, making selective redundancy unlikely.

One approach to understanding the cell-specific effects of the loss of Brn3a expression is suggested by recent work in which we have demonstrated a correlation between Brn3a binding to its target sites *in vivo* and H3-acetylation in the vicinity of the potential binding sites [[27] in press]. Given these results, one potential mechanism for the differential regulation of target genes by Brn3a might be distinct modifications of chromatin at the target gene loci in the DRG and TG, which could modulate the effects of Brn3a or downstream regulatory factors. To examine this question for the differentially regulated loci *Tcfap2b*, *NeuroD4* and *Gata3*, we used chromatin immunoprecipitation (ChIP) to profile histone H3 acetylation in wild-type E13.5 DRG and TG (Figure 7). We also examined the *Msc* locus as an example of a gene that shows similarly increased expression in the DRG and TG of Brn3a knockout mice. ChIP assays of the promoter regions of three constitutively expressed genes, *Gapdh*, *Mapt* (*tau*), and *Eno2* (neuron specific enolase), were used as positive con-

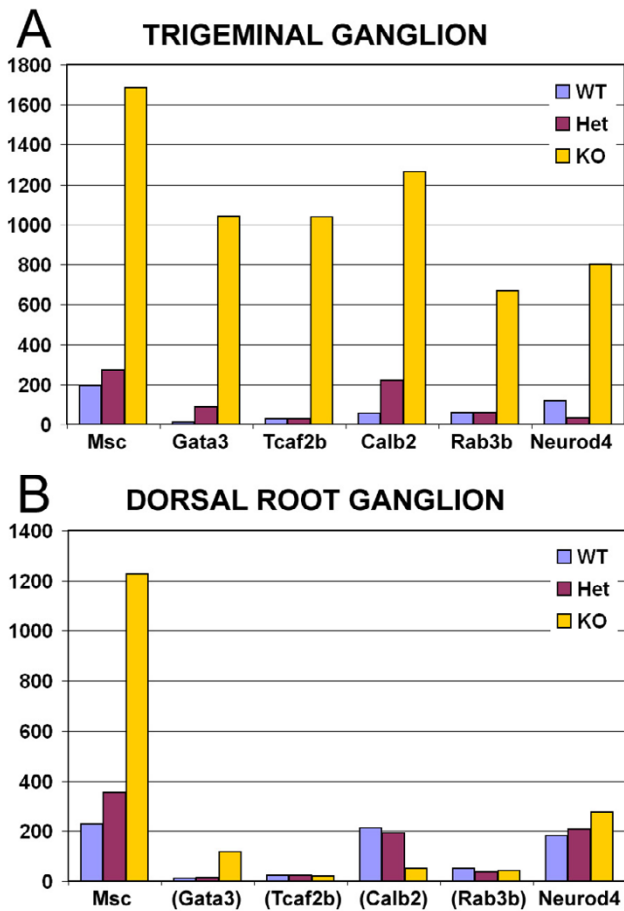


Figure 6
Trigeminal-specific targets of Brn3a regulation. **(a)** TG data from a previously published data set [20]. **(b)** DRG data from the present study. Brn3a wild-type (WT), heterozygote (Het) and knockout (KO) E13.5 DRG were analyzed for global gene expression using U74Av2+U74v2B arrays to allow direct comparison with the prior analysis of the embryonic TG (Additional file 3). *Msc*, shown for comparison, exhibits markedly increased expression in the DRG and TG of Brn3a knockout mice, while *Gata3*, *Tcfap2b*, *Calb2*, *Rab3b* and *Neurod4* are increased only in the DRG. Changes in *Msc*, *Gata3*, *Tcfap2b*, *Calb2* and *Neurod4* have been previously verified in the TG of Brn3a knockout mice by *in situ* hybridization or immunofluorescence [20]. *Rab3b* is newly identified as a Brn3a target in the TG due to progress in the annotation of the mouse genome. Gene abbreviations in parentheses indicate expression below the statistically significant threshold of detection (absent call) in all three genotypes.

controls, and the results were normalized to negative control assays from the promoter region of the *Alb1* (albumin) gene, which is not expressed in the nervous system. Because the genomic sequences that regulate these genes in the sensory ganglia have not been defined, we surveyed histone acetylation across these loci using multiple oligo-

nucleotide pairs spaced at 500 to 1,000 base-pair (bp) intervals from approximately -10 kb to +15 kb relative to the start of transcription, using quantitative real-time PCR ("locus-ChIP") ["locus-ChIP", [27] in press].

ChIP profiling of the *Msc* locus revealed similar levels of H3-acetylation in the DRG and TG. However, ChIP assays of the *Tcfap2b* and *NeuroD4* loci revealed significantly greater H3-acetylation in the TG relative to the DRG ($p = 0.0003$ and $p = 0.0005$, respectively), while the *Gata3* locus exhibited a trend ($p = 0.09$) toward greater acetylation in the TG. As expected, the positive control promoters were highly acetylated, and the negative control, *Alb1*, was deacetylated in both the DRG and TG. Thus, the state of H3-acetylation in wild-type ganglia appears to be correlated both with basal expression and also with a state of latent potential expression that can be induced in Brn3a null ganglia.

Discussion

Numerous transcription factors have been shown to play key roles in the differentiation of brainstem, spinal, and spinal sensory neurons, yet, for the most part, the programs of gene expression regulated by these factors remain unknown. A layer of complexity is added to the analysis of the downstream targets of these factors by the fact that their expression patterns are often very complex, and may include diverse classes of neurons and non-neuronal cell types with no obvious common characteristics. Brn3a, for example, is expressed in a majority of differentiating peripheral sensory neurons, and also in specific neurons of the spinal cord, olivo-cerebellar system, mid-brain, diencephalon and retina. The LIM-domain transcription factor *Islet1* is co-expressed with Brn3a in the sensory system [10], but in the CNS it is expressed primarily in motor neurons [28,29], and also has important roles in the development of the heart [30] and pancreatic islet cells [31]. A fundamental unanswered question is whether these factors, and many others with expression patterns of similar complexity, regulate the same downstream targets in different neuronal types, and in neurons versus non-neuronal cells.

To better understand the molecular pathways of sensory development, we initiated the present study by examining global gene expression in the brachial-level DRG and TG at E13.5. At this stage, when essentially all sensory neurons have exited the cell cycle and markers of sensory subtypes are beginning to be expressed, the gene expression patterns of the DRG and TG are quite similar. Some transcripts exhibit quantitative differences between the ganglia, which may represent relative differences in cellular composition or the timetable of development, but very few transcripts are uniquely expressed in either the DRG or TG. Most prominent among the few transcripts

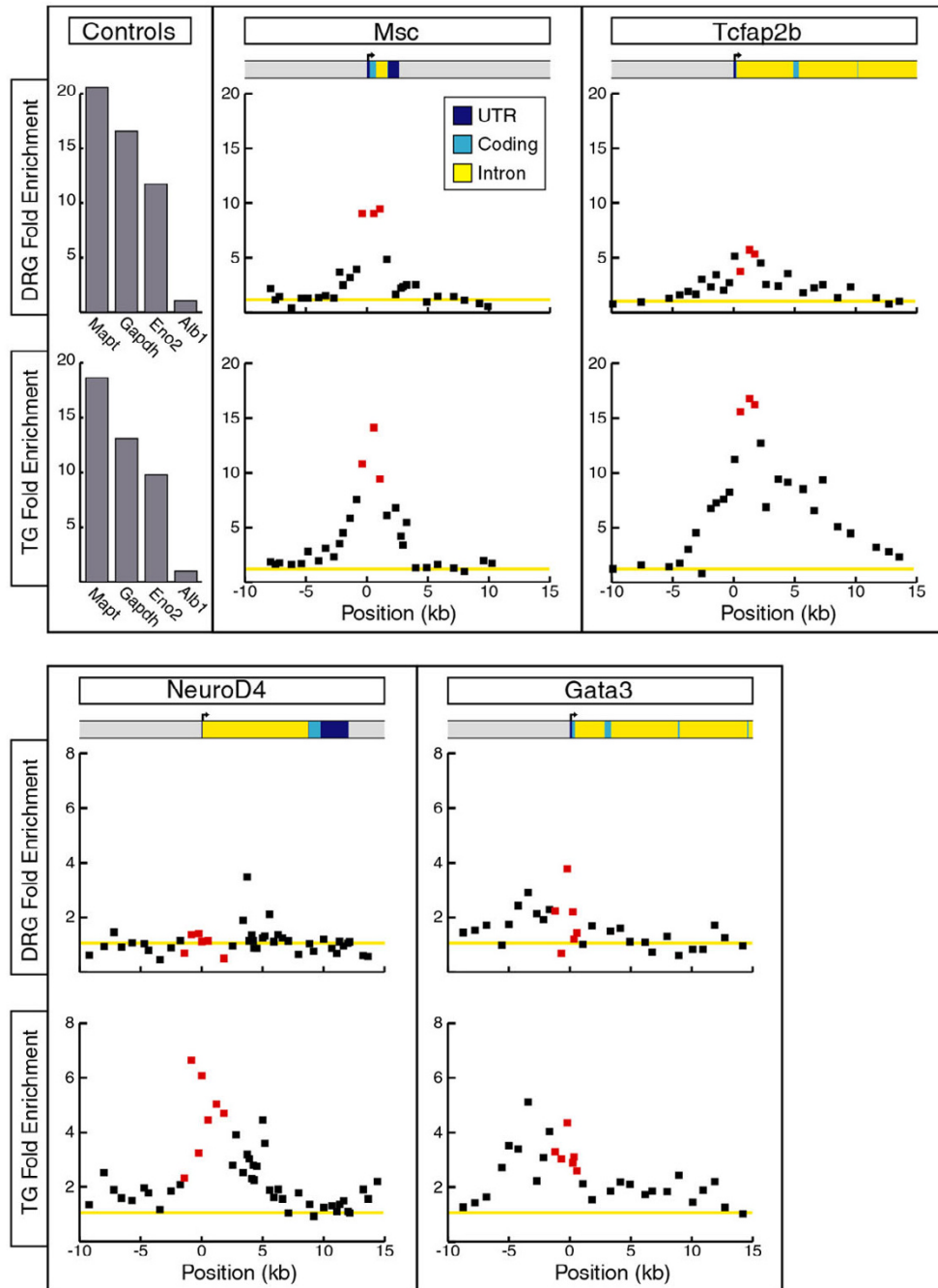


Figure 7

Acetyl-histone H3 profiling of Brn3a target gene loci. Histone H3 acetylation was assayed using ChIP and tiled PCR primer pairs from -10 kb to 15 kb of the *Msc*, *Tcfap2b*, *NeuroD4* and *Gata3* gene loci. Positive controls for these assays included primer pairs located in the promoter regions of the *Mapt* (*tau*), *Gapdh*, and *Eno2* loci, which are highly expressed in the DRG and TG and are unchanged in Brn3a null mice. The silent *alb1* locus was used as a negative control and to set the baseline of one-fold enrichment (yellow line). H3 acetylation of these loci in chromatin samples from the E13.5 DRG and TG were compared by *t*-tests using fold enrichment values for primer pairs flanking the transcription start site of each locus (points shown in red). H3 acetylation was not significantly different at the *msc* locus ($p = 0.25$), while *Tcfap2b* ($p = 0.0003$) and *NeuroD4* ($p = 0.0005$) showed significantly greater acetylation in the TG, and *Gata3* ($p = 0.09$) showed a trend toward greater acetylation in the TG. UTR, untranslated region.

restricted to a particular axial level are those encoded by the *Hox* genes and *Etv1*, which at this stage are expressed only in the DRG. The restriction of the *Hox* transcripts (with the exception of *HoxD1*) to spinal levels is expected based on the well characterized axial expression pattern of these genes. *Etv1* expression is restricted to the DRG at E13.5 because the first neurons to express this marker, the large proprioceptive neurons innervating muscle spindles, develop within the DRG at spinal levels but at cranial levels are largely sequestered in the mesV. *Etv1*-expressing neurons that develop in the TG by E16.5 are distinguished by smaller size and the co-expression of *Islet2*, and appear to represent a distinct subset of sensory neurons.

Global analysis of gene expression in *Brn3a* knockout and wild-type DRG demonstrates that *Brn3a* regulates, directly or indirectly, an extensive program of gene expression. Advances in microarray technology and in the annotation of the mouse genome have allowed us to significantly expand the number of identified *Brn3a* targets from a prior study of the TG [20]. A large number of the downstream targets of *Brn3a* in the DRG have known roles in neurogenesis or neural function, and include components of axons and synapses, neurotransmitters and their receptors, mediators of intracellular signaling, and transcription factors. Because the regulatory sequences of many of these genes have not been described, in many cases it is not possible to distinguish direct regulatory targets from secondary or compensatory effects. However, in recent studies we have used locus-ChIP to demonstrate that *Brn3a* is a direct repressor of *NeuroD1* and *NeuroD4* in the embryonic TG [[27] in press], as well as a negative modulator of its own expression [32,33].

Most *Brn3a* target genes are conserved between sensory neurons at cranial and spinal levels. However, a subset of genes with the most increased expression in the TG do not change expression in the *Brn3a* knockout DRG, and are generally undetectable in the E13.5 DRG of animals of any genotype. These differentially regulated transcripts include the transcription factors *Tcfap2b*, *Gata3* and *NeuroD4*, the calcium binding protein calbindin2 (calretinin), and the small GTP-binding protein *Rab3b*, implicated in synaptic vesicle release [34]. Because there are normally few transcripts that distinguish the TG from the DRG at this stage of development, the gene expression patterns of the DRG and TG are significantly more different in *Brn3a* knockout ganglia than in the wild type. This suggests that one important role for *Brn3a* is to suppress potential differences in gene expression between the spinal and cranial ganglia, mediating a process of 'convergent development' in which functionally similar populations of neurons are generated from different embryological sources.

The state of histone H3 acetylation of *Brn3a* target gene loci offers some insight into the underlying mechanism of the differential regulation of these targets at spinal and cranial levels. Normally, H3 acetylation is associated with the regulatory sequences in the promoters of actively transcribed genes. Consistent with this, we have previously shown that the promoter region of *Pou4f1* itself is highly acetylated in the TG, and the promoters of genes that are silent in the sensory ganglia regardless of *Brn3a* genotype are deacetylated [[27] in press]. In wild-type DRG and TG, the differentially regulated genes *NeuroD4* and *Tcfap2b* are nearly silent, yet these gene loci can be distinguished in trigeminal neurons by increased H3 acetylation over a region encompassing the transcription start site. The *Msc* gene is also normally silent, but it exhibits increased expression at both cranial and spinal levels in *Brn3a* null mice, and is accordingly H3 acetylated in both the DRG and TG. Thus, in the case of these genes with increased expression in the *Brn3a* knockout, H3 acetylation appears to reveal a latent state of potential expression, which is normally repressed by *Brn3a* or its downstream effectors, and de-repressed in *Brn3a* knockout ganglia.

The failure of DRG neurons to increase *NeuroD4* and *Tcfap2b* expression in *Brn3a* knockout ganglia suggests that a redundant mechanism of repression exists for these genes at spinal but not cranial levels. The action of such a repressor may be reflected in the low levels of histone acetylation at these loci in the DRG. Because the most prominent distinguishing feature of sensory gene expression at spinal levels is the expression of multiple *Hox* genes, these factors are candidate mediators of this selective repression of *NeuroD4* and *Tcfap2b* in the DRG. Transcriptional repressor functions have been described for the *Hox* genes [35], and there is evidence that *Hox* proteins can directly block the activity of the widely expressed histone acetyltransferase CBP-p300 [36]. *Hox* gene repression of a subset of *Brn3a* target gene loci could be an active process at E13.5, or *Hox* gene expression at earlier developmental stages could produce persisting modifications of chromatin, reflected in the deacetylation of these loci observed here, resulting in reduced transcription even when direct repression by *Hox* genes is no longer active.

Materials and methods

Matings, embryos, and RNA isolation for array analysis

To generate tissue for microarray analysis, timed matings of *Brn3a* heterozygote animals were performed, and the embryos were harvested at E13.5. Only embryos corresponding to E13.5 \pm 0.5 days based on the staging system of Theiler [37] were used for microarray analysis. TG were removed by blunt dissection and carefully freed of adherent non-neural tissue with fine forceps. DRG were isolated by stripping of the spinal cord with its adherent ganglia, followed by dissection of the ganglia with fine forceps.

DRG were harvested from brachial region only, including the C5-T1 levels. Dissected ganglia were placed in RNase inhibitor solution (RNAlater, Ambion, Austin TX), and RNA was prepared using the RNeasy system (Qiagen, Valencia, CA). Embryos were genotyped for Brn3a alleles as previously described [17] from a sample of tail or hind-limb tissue harvested at the time of ganglion dissection. Genotyped TG or DRG from five embryos were sufficient to provide approximately 5 µg of total RNA for a single microarray analysis. The generation of cDNA, production of labeled cRNA, and hybridization to GeneChip arrays were all performed according to standard protocols provided by the manufacturer (Affymetrix, Santa Clara, CA).

Analysis of expression array data

The principal microarray datasets presented here for the mouse DRG and TG were generated using the Affymetrix 430A and 430B microarrays. In addition, the same DRG samples were analyzed using Affymetrix U74A and U74B arrays for direct comparison with prior data sets for the TG [20]. The primary analysis of microarray data, including determination of the absence/presence of the assayed transcripts, transcript expression levels, and the probability of change in transcript expression between samples ('change p ') was performed with Microarray Suite 5.0 (Affymetrix). Default Microarray Suite 5.0 parameters were used for increase (I) and decrease (D) calls. For the 430 array set these cutoff values were $p < 0.005$ and $p > 0.995$ for I and D, respectively, and for the U74 arrays, the values were $p < 0.003$ and $p > 0.997$. All array values were initially scaled to a mean value of 500 using global scaling. To permit more meaningful comparison of the expression levels of transcripts assayed by the 430A and 430B arrays, the initial expression values for the 430B array were rescaled based on the expression levels of 100 probe sets in common between the 430A and 430B arrays. Microarray probe sets were related to the corresponding mouse transcripts using the NetAffx database (Affymetrix), based on the NCBI Build 34 annotation of the mouse genome. The array data discussed in this publication have been deposited in NCBI's Gene Expression Omnibus (GEO) [38] and are accessible through GEO series accession number GSE5658.

Comparisons of gene expression between wild-type DRG and TG (Table 1) and between the DRG from Brn3a wild-type, heterozygous, and knockout mice (Tables 2 and 3) were performed in duplicate, using separate pools of isolated ganglia. To be included in the tables of changed transcripts for a given tissue or genotype, the following criteria were met: both replicates were called as 'present' in the condition of greater expression; both replicates exhibited an increased or 'I' call for the condition of higher expression; and the probe set identified an annotated and named transcript in NCBI Build 34 of the mouse genome.

Duplicate probe sets identifying the same transcript were eliminated, and the tables are annotated with the number of concordant probe sets for each transcript. Concordance was identified by the agreement of the present and increased calls for the duplicate probe set, and a minimum fold change of 2.0. In the case of multiple concordant probe sets, the probe set with the greatest fold change is listed in the tables. Results for the probe sets meeting the inclusion criteria were ranked by fold change, and the cutoff value for inclusion appears in the tables.

In situ hybridization and immunofluorescence

Non-isotopic *in situ* hybridization was performed as previously described [38]. A list of probes used and their sources appears in additional file 5. Immunofluorescence for Brn3a was performed with rabbit polyclonal antisera as previously as previously described [39]. Other antisera used included rabbit antisera against Etv1/Er81 and Runx3 obtained from Dr Sylvia Arber [13,15], and guinea pig antisera against Islet2, obtained from Dr Sam Pfaff [28]. Immunofluorescence for other antigens was performed with commercially available antibodies, including rabbit anti-calretinin (Swant, Bellinzona, Switzerland), rabbit anti-galanin (Bachem, King of Prussia, PA), rabbit anti-somatostatin-14 (Peninsula Laboratories), and goat anti-β-galactosidase (Biogenesis (MorphoSys), Kingston, NH).

Locus-wide chromatin immunoprecipitation

Locus-ChIP assays were performed as previously described [[27] in press]. In brief, embryos for ChIP assays were generated from timed matings of ICR mice. DRG and TG were dissected from E13.5 embryos and fixed in 4% paraformaldehyde for 30 minutes, then quenched with 150 mM glycine. The fixed tissue was washed with phosphate-buffered saline and stored at -80°C until analysis.

Selection of chromatin complexes from embryonic sensory ganglia was performed by a modification of a widely used procedure [40]. For each analysis, fixed ganglia from 30 embryos (60 TG or approximately 300 DRG) were pooled and suspended in lysis buffer containing 50 mM Tris-HCl, pH 8.1, with 10 mM EDTA and 1% SDS, 1 mM 4-(2-Aminoethyl)benzenesulfonyl fluoride, HCl (AEBSF) and a proprietary protease inhibitor mix (1 × Complete Mini, Roche, Indianapolis, IN; used according to instructions). Chromatin was then fragmented to an average size of 500 bp by sonication, and insoluble cellular debris was removed by centrifugation. The supernatant containing fragmented chromatin was diluted in 15 mM Tris-HCl, pH 8.1, with 150 mM NaCl, 1 mM EDTA, 1% Triton-X-100, 0.01% SDS, and protease inhibitor mix. An unselected ('input') sample of 10% of the total homogenate was removed prior to antibody selection.

ChIP was performed using rabbit anti-acetylated histone H3 antibody (Upstate Biotechnology, Inc., Bellerica, MA, catalog no. 06-599), which recognizes histone H3 acetylated at lys9 and lys14. For each selection, 50 µg of anti-histone antibody was coupled to 250 µL of anti-rabbit IgG magnetic beads (DynaM-280), in lysis buffer containing 50 mM Tris-HCl, pH 8.1, with 10 mM EDTA and 1% SDS. To reduce non-specific background, the chromatin sample was pre-cleared using the magnetic beads with the secondary antibody alone. The sample was then incubated overnight with secondary antibody-coupled beads to select the acetyl H3-containing chromatin complexes. The beads were then washed for 5 minutes at room temperature with each of the following solutions: 20 mM Tris-HCl, pH 8.1, with 150 mM NaCl, 2 mM EDTA, 0.1 % SDS, and 1% Triton-X-100; 20 mM Tris-HCl, pH 8.1, with 500 mM NaCl, 2 mM EDTA, 0.1% SDS, and 1% Triton-X-100; 10 mM Tris-HCl, pH 8.1, with 1 mM EDTA, 0.25 M LiCl, 1% NP-40, and 1% deoxycholate. Salt and detergent were removed by washing twice with 10 mM Tris-HCl, 1 mM EDTA, pH 8. DNA was extracted from the antibody-chromatin complexes and the input sample by heating in 0.1 M NaHCO₃ with 200 mM NaCl and 1% SDS at 65°C for 4 hours with constant shaking. The input and selected samples were then digested with proteinase K, extracted with phenol/chloroform, and precipitated with ethanol.

Real-time locus-wide PCR analysis

Chromatin fragments recovered from the immunoprecipitated and input samples were then assayed by real-time PCR using an ABI 7300 thermocycler and SYBR Green fluorimetric detection. To screen an entire gene locus, oligonucleotide pairs were designed at 500 to 1,000 bp intervals throughout the region, and selected and unselected samples were run in parallel in a 96-well plate format. The primer pairs used for locus-ChIP assays of the *NeuroD4*, *Msc*, *Tcfap2b* and *Gata3* loci appear in additional file 5.

The enrichment of immunoprecipitated chromatin fragments was assayed by the cycle-threshold difference method [41]. For this method, real-time PCR signals are measured using the 'cycle threshold', or Ct parameter, which is the number of cycles required for the amplification product to reach an arbitrary level of fluorescence intensity (threshold), and is logarithmic to the initial abundance of the target sequence in the sample. For each PCR amplicon, a ΔCt value comparing the unselected (input) and antibody-selected DNA samples was then calculated by subtracting the Ct_{selected} from the Ct_{input} signal:

$$\Delta Ct = Ct_{\text{input}} - Ct_{\text{selected}}$$

Fold enrichment values for target sequences bound by the selecting antibodies, corresponding to the y-axis of the

locus-ChIP plots, were calculated using the following equation:

$$E = 2^{(\Delta Ct - \Delta Ct_{\text{control}})}$$

Because product formation approximately doubles with each cycle in the linear range of amplification, a ΔCt of one cycle represents a two-fold difference in starting template. A significant advantage of this method is that, for each primer pair, a selected sample is compared directly to its unselected control, which differs only by the antibody selection process. Potentially confounding factors such as small differences in the PCR amplification efficiency of different primer pairs are eliminated in this comparison.

The ΔCt assays for each pool of selected material were normalized to an arbitrary baseline (one-fold enrichment) determined using two primer pairs in the promoter region of the *Alb1* (albumin locus), which was chosen as a negative control because it is not transcribed in the nervous system. Fold enrichment values for the *Alb1* locus were very similar to values for the unselected, intergenic regions of the target gene loci. Primer pairs in the promoter regions of *Mapt* (microtubule-associated protein tau) and *Eno2* (neuron specific enolase), which exhibit tissue specific expression in the nervous system, and *Gapdh* (glyceraldehyde-3-phosphate dehydrogenase), which is expressed ubiquitously, were used as positive controls. Comparisons of histone H3 acetylation at a given locus in the DRG and TG were made using three- to six-fold enrichment values using oligonucleotide pairs in a contiguous genomic region near the transcription start site of the analyzed gene loci. The statistical significance (*p* values) of the difference in H3 acetylation was determined using two-sample, unequal variance *t*-tests.

Competing interests

The author(s) declare that they have no competing interests.

Additional material

Additional file 1

Differential gene expression in trigeminal and dorsal root ganglia. In situ hybridization showing transcripts differentially expressed in the trigeminal and dorsal root ganglia.

Click here for file

[<http://www.biomedcentral.com/content/supplementary/1749-8104-2-3-S1.doc>]

Additional file 2

Increased and Decreased transcripts in E13.5 DRG of Brn3a knockout mice. This shows a more complete version of the data set presented in Table 1.

Click here for file

[<http://www.biomedcentral.com/content/supplementary/1749-8104-2-3-S2.doc>]

Additional file 3

Direct comparison of altered gene expression in DRG and TG of Brn3a knockout sensory ganglia. Gene expression in the DRG is analyzed using the U74v2 array set to allow direct comparison to a prior data set for the TG.

Click here for file

[<http://www.biomedcentral.com/content/supplementary/1749-8104-2-3-S3.doc>]

Additional file 4

Dorsal root ganglia exhibit significant compensation for the loss of one Brn3a allele. Gene expression levels are compared for Brn3a wild-type, heterozygote, and knockout ganglia to demonstrate the extent to which gene dosage compensation reduces the heterozygote phenotype.

Click here for file

[<http://www.biomedcentral.com/content/supplementary/1749-8104-2-3-S4.doc>]

Additional file 5

Summary of in situ hybridization probes and Locus-ChIP oligonucleotides. Summary of in situ hybridization probes and Locus-ChIP oligonucleotides.

Click here for file

[<http://www.biomedcentral.com/content/supplementary/1749-8104-2-3-S5.doc>]

Acknowledgements

We would like to acknowledge Bill Wachsmann and Lutfunnessa Shireen for assistance with microarray technology. Dr Sylvia Arber generously provided antisera for Runx3 and ETV1/Er81, and Islet2 antiserum was the generous gift of Dr Sam Pfaff. We would also like to thank Drs Jean-Francois Brunet, Allan Basbaum, Ryoichiro Kageyama, Nobuyuki Itoh, Eric Olson and their associates for *in situ* hybridization probes. Microarray data used in this study are deposited in the Gene Expression Omnibus, series accession number GSE5658. Supported in part by Department of Veterans Affairs MERIT funding and VISN 22 MIRECC (EET), and NIH awards HD33442 and MH065496. EET and NF are a NARSAD Investigators.

References

- Anderson DJ: **Lineages and transcription factors in the specification of vertebrate primary sensory neurons.** *Current Opinion in Neurobiology* 1999, **9**:517-524.
- Shirasaki R, Pfaff SL: **Transcriptional codes and the control of neuronal identity.** *Annu Rev Neurosci* 2002, **25**:251-281.
- Baker CV, Bronner-Fraser M: **Vertebrate cranial placodes I. Embryonic induction.** *Dev Biol* 2001, **232**:1-61.
- Le Douarin NM, Smith J: **Development of the peripheral nervous system from the neural crest.** *Annu Rev Cell Biol* 1988, **4**:375-404.
- Lazarov NE: **Comparative analysis of the chemical neuroanatomy of the mammalian trigeminal ganglion and mesencephalic trigeminal nucleus.** *Prog Neurobiol* 2002, **66**:19-59.
- Hunter E, Begbie J, Mason I, Graham A: **Early development of the mesencephalic trigeminal nucleus.** *Dev Dyn* 2001, **222**:484-493.
- Ma Q, Fode C, Guillemot F, Anderson DJ: **Neurogenin1 and neurogenin2 control two distinct waves of neurogenesis in developing dorsal root ganglia.** *Genes Dev* 1999, **13**:1717-1728.
- Ma Q, Chen Z, Barrantes I, de la Pompa JL, Anderson DL: **Neurogenin1 is essential for the determination of neuronal precursors for proximal sensory ganglia.** *Neuron* 1998, **20**:469-482.
- Fode C, Gradwohl G, Morin X, Dierich A, LeMeur M, Goridis C, Guillemot F: **The bHLH protein Neurogenin2 is a determination factor for epibranchial placode-derived sensory neurons.** *Neuron* 1998, **20**:483-494.
- Fedtsova N, Perris R, Turner EE: **Sonic hedgehog regulates the position of the trigeminal ganglia.** *Dev Biol* 2003, **261**:456-469.
- Chen ZF, Rebelo S, White F, Malmberg AB, Baba H, Lima D, Woolf CJ, Basbaum AI, Anderson DJ: **The paired homeodomain protein DRG11 is required for the projection of cutaneous sensory afferent fibers to the dorsal spinal cord.** *Neuron* 2001, **31**:59-73.
- Chen CL, Broom DC, Liu Y, de Nooij JC, Li Z, Cen C, Samad OA, Jessell TM, Woolf CJ, Ma Q: **Runx1 Determines Nociceptive Sensory Neuron Phenotype and Is Required for Thermal and Neuropathic Pain.** *Neuron* 2006, **49**:365-377.
- Arber S, Ladle DR, Lin JH, Frank E, Jessell TM: **ETS gene Er81 controls the formation of functional connections between group Ia sensory afferents and motor neurons.** *Cell* 2000, **101**:485-498.
- Levanon D, Bettoun D, Harris-Cerruti C, Woolf E, Negreanu V, Eilam R, Bernstein Y, Goldenberg D, Xiao C, Fliedrauf M, Kremer E, Otto F, Brenner O, Lev-Tov A, Groner Y: **The Runx3 transcription factor regulates development and survival of TrkC dorsal root ganglia neurons.** *Embo J* 2002, **21**:3454-3463.
- Kramer I, Sigris M, de Nooij JC, Taniuchi I, Jessell TM, Arber S: **A Role for Runx Transcription Factor Signaling in Dorsal Root Ganglion Sensory Neuron Diversification.** *Neuron* 2006, **49**:379-393.
- McEvelly RJ, Erkman L, Luo L, Sawchenko PE, Ryan AF, Rosenfeld MG: **Requirement for Brn-3.0 in differentiation and survival of sensory and motor neurons.** *Nature* 1996, **384**:574-577.
- Eng SR, Gratwick K, Rhee JM, Fedtsova N, Gan L, Turner EE: **Defects in sensory axon growth precede neuronal death in Brn3a-deficient mice.** *J Neurosci* 2001, **21**:541-549.
- Xiang M, Lin G, Zhou L, Klein WH, Nathans J: **Targeted deletion of the mouse POU-domain gene Brn-3a causes a selective loss of neurons in the brainstem and trigeminal ganglion, uncoordinated limb movement, and impaired suckling.** *Proc Natl Acad Sci* 1996, **93**:11950-11955.
- Huang EJ, Zang K, Schmidt A, Saulys A, Xiang M, Reichardt LF: **POU domain factor Brn-3a controls the differentiation and survival of trigeminal neurons by regulating Trk receptor expression.** *Development* 1999, **126**:2869-2882.
- Eng SR, Lanier J, Fedtsova N, Turner EE: **Coordinated regulation of gene expression by Brn3a in developing sensory ganglia.** *Development* 2004, **131**:3859-3870.
- Patel TD, Kramer I, Kucera J, Niederkofler V, Jessell TM, Arber S, Snider WD: **Peripheral NT3 signaling is required for ETS protein expression and central patterning of proprioceptive sensory afferents.** *Neuron* 2003, **38**:403-416.
- Raappana P, Arvidsson J: **Location, morphology, and central projections of mesencephalic trigeminal neurons innervating rat masticatory muscles studied by axonal transport of cholera toxin B-subunit horseradish peroxidase.** *J Comp Neurol* 1993, **328**:103-114.
- Jin M, Ishida M, Katoh-Fukui Y, Tsuchiya R, Higashinakagawa T, Ikegami S, Arimatsu Y: **Reduced pain sensitivity in mice lacking latxin, an inhibitor of metalloproteinases.** *Brain Res* 2006, **1075**:117-121.
- Demyanenko GP, Schachner M, Anton E, Schmid R, Feng G, Sanes J, Maness PF: **Close homolog of L1 modulates area-specific neuronal positioning and dendrite orientation in the cerebral cortex.** *Neuron* 2004, **44**:423-437.
- Nelson BR, Claes K, Todd V, Chaverra M, Lefcort F: **NELL2 promotes motor and sensory neuron differentiation and stimulates mitogenesis in DRG in vivo.** *Dev Biol* 2004, **270**:322-335.
- Shibata M, Ishii J, Koizumi H, Shibata N, Dohmae N, Takio K, Adachi H, Tsujimoto M, Arai H: **Type F scavenger receptor SREC-1 interacts with advillin, a member of the gelsolin/villin family,**

- and induces neurite-like outgrowth. *J Biol Chem* 2004, **279**:40084-40090.
27. Lanier J, Quina LA, Eng SR, Cox E, Turner EE: **Brn3a target gene recognition in embryonic sensory neurons.** *Developmental Biology* **In Press, Accepted Manuscript**.
 28. Thaler JP, Koo SJ, Kania A, Lettieri K, Andrews S, Cox C, Jessell TM, Pfaff SL: **A postmitotic role for Isl-class LIM homeodomain proteins in the assignment of visceral spinal motor neuron identity.** *Neuron* 2004, **41**:337-350.
 29. Pfaff SL, Mendelsohn M, Stewart CL, Edlund T, Jessell TM: **Requirement for LIM homeobox gene Isl1 in motor neuron generation reveals a motor neuron-dependent step in interneuron differentiation.** *Cell* 1996, **84**:309-320.
 30. Cai CL, Liang X, Shi Y, Chu PH, Pfaff SL, Chen J, Evans S: **Isl1 identifies a cardiac progenitor population that proliferates prior to differentiation and contributes a majority of cells to the heart.** *Dev Cell* 2003, **5**:877-889.
 31. Ahlgren U, Pfaff SL, Jessell TM, Edlund T, Edlund H: **Independent requirement for ISL1 in formation of pancreatic mesenchyme and islet cells.** *Nature* 1997, **385**:257-260.
 32. Trieu M, Ma A, Eng SR, Fedtsova N, Turner EE: **Direct autoregulation and gene dosage compensation by POU-domain transcription factor Brn3a.** *Development* 2003, **130**:111-121.
 33. Trieu M, Rhee JM, Fedtsova N, Turner EE: **Autoregulatory sequences are revealed by complex stability screening of the mouse brn-3.0 locus.** *J Neurosci* 1999, **19**:6549-6558.
 34. Schluter OM, Schmitz F, Jahn R, Rosenmund C, Sudhof TC: **A complete genetic analysis of neuronal Rab3 function.** *J Neurosci* 2004, **24**:6629-6637.
 35. Svingen T, Tonissen KF: **Hox transcription factors and their elusive mammalian gene targets.** *Heredity* 2006, **97**:88-96.
 36. Shen WF, Krishnan K, Lawrence HJ, Largman C: **The HOX homeodomain proteins block CBP histone acetyltransferase activity.** *Mol Cell Biol* 2001, **21**:7509-7522.
 37. Theiler K: **The house mouse; development and normal stages from fertilization to 4 weeks of age.** Berlin, New York, Springer-Verlag; 1972:168.
 38. Birren SJ, Lo L, Anderson DJ: **Sympathetic neuroblasts undergo a developmental switch in trophic dependence.** *Development* 1993, **119**:597-610.
 39. Fedtsova N, Turner EE: **Brn-3.0 Expression identifies early postmitotic CNS neurons and sensory neural precursors.** *Mechanisms of Development* 1995, **53**:291-304.
 40. Luo RX, Postigo AA, Dean DC: **Rb interacts with histone deacetylase to repress transcription.** *Cell* 1998, **92**:463-473.
 41. Livak KJ, Schmittgen TD: **Analysis of relative gene expression data using real-time quantitative PCR and the 2(-Delta Delta C(T)) Method.** *Methods* 2001, **25**:402-408.
 42. Quina LA, Pak W, Lanier J, Banwait P, Gratwick K, Liu Y, Velasquez T, O'Leary DD, Goulding M, Turner EE: **Brn3a-expressing retinal ganglion cells project specifically to thalamocortical and collicular visual pathways.** *J Neurosci* 2005, **25**:11595-11604.
 43. Grillet N, Dubreuil V, Dufour HD, Brunet JF: **Dynamic expression of RGS4 in the developing nervous system and regulation by the neural type-specific transcription factor Phox2b.** *J Neurosci* 2003, **23**:10613-10621.
 44. Polizzotto MN, Bartlett PF, Turnley AM: **Expression of "suppressor of cytokine signalling" (SOCS) genes in the developing and adult mouse nervous system.** *J Comp Neurol* 2000, **423**:348-358.

Publish with **BioMed Central** and every scientist can read your work free of charge

"BioMed Central will be the most significant development for disseminating the results of biomedical research in our lifetime."

Sir Paul Nurse, Cancer Research UK

Your research papers will be:

- available free of charge to the entire biomedical community
- peer reviewed and published immediately upon acceptance
- cited in PubMed and archived on PubMed Central
- yours — you keep the copyright

Submit your manuscript here:
http://www.biomedcentral.com/info/publishing_adv.asp

